*Int. J. Heat Mass Transfer.* Vol. 34, No. 11, pp. 2715–2726, 1991
Printed in Great Britain

0017–9310/91 $3.00 + 0.00


# Thermal dispersion in thick-walled tubes as a model of porous media

ZENG-GUANG YUAN, WILBUR H. SOMERTON and KENT S. UDELL†
Department of Mechanical Engineering, University of California, Berkeley, CA 94720, U.S.A.

(*Received* 18 *April* 1990 *and in final form* 18 *December* 1990)

**Abstract**—A theoretical study of thermal dispersion in porous media is presented. The contribution of pore level velocity distributions on dispersion is captured in an analysis of thermal transport in a thick-walled tube containing a flowing fluid. It is shown that the cases of an applied steady-state temperature gradient and a traveling temperature wave produce different thermal dispersivities. In both cases, the dispersion coefficient is defined by the static thermal conductivity plus a term due to dispersive flow. The dispersive term is proportional to the Peclet number squared. The proportionality coefficient is shown to be a function of porosity, fluid and solid thermal properties, and the temperature field. Through consideration of a bundle of tubes of various radii, the contribution of heterogeneities on thermal dispersion is evaluated. Variations of pore diameters are shown to cause orders of magnitude increases in dispersion.

Satisfactory comparisons of the dispersion model with published experimental data are presented.

## 1. INTRODUCTION

KNOWLEDGE of the thermal dispersion coefficients for porous media saturated with flowing fluids is of fundamental importance in a wide variety of engineering applications such as thermal oil recovery, geothermal energy recovery, heat transfer in packed beds, etc. The phenomenon of transport in porous media is extremely complicated due to the complex pore geometries. A common approach to problems regarding heat or mass transfer in porous media is to treat the medium as a continuum where the domain of interest is substantially greater than the characteristic pore size and grain size of the medium. Application of the principle of conservation of energy to a control volume of the pseudo-continuum yields the following energy equation in which radiation and viscous dissipation effects are negligible:

$$\nabla\cdot(\lambda_d\nabla T)-\nabla\cdot(\rho_f c_f \mathbf{v}_d T) = [\rho_f c_f\phi+\rho_s c_s(1-\phi)]\frac{\partial T}{\partial t} \quad (1)$$

where $\lambda_d$ is the thermal dispersion coefficient, or effective thermal conductivity, and $\mathbf{v}_d$ the Darcy velocity. The apparent advantage of this approach is its simplicity in that there is no need to distinguish the fluid phase from the solid phase in the medium. But what accompanies this simplification are the difficulties in defining $\lambda_d$ and $T$. The role of $\lambda_d$ in equation (1) is the same as that of thermal conductivity in the energy equation of a true continuum. Strictly speaking, Fourier's law does not apply to the presumed continua of porous media. The thermal conductivity of a fluid or a solid defined by Fourier's law is an inherent physical property of the material independent of its velocity of motion. However, the thermal dispersion coefficient $\lambda_d$ of a porous medium saturated with fluids behaves in quite a different manner, in that it depends on the velocities of the fluids within it. For this reason, $\lambda_d$ is better named a thermal dispersion coefficient than effective thermal conductivity.

A considerable amount of effort has been made to correlate thermal dispersion coefficients with other properties of the porous medium. In the early 1960s, Kunii and Smith, along with other researchers [1–4], conducted extensive experimental investigations of the thermal dispersion coefficient for a one-dimensional porous rock and packed beds of unconsolidated sands or glass beads under steady-state fluid flow conditions. In those experiments, a heat source and a heat sink were placed at either end of the bed. Fluids were flowed through the medium in the opposite direction to the heat flux. Similar experiments were also performed on sandstones. Kunii and Smith found that the thermal dispersion coefficient increased significantly with mass velocity of the fluids. Other interesting work by Willhite *et al.* [3] showed that when the fluid flowed in the direction perpendicular to the heat flux, there was no effect of the flow velocity on the thermal diffusivities over the range of modified Reynolds number from 0 to 6.6.

In addition to the steady-state experiments reported above, a number of experimental investigations under transient conditions have been reported [5–7]. In the early 1960s Green *et al.* [5] carried out experiments observing the response of packed beds to a step change in temperature of the fluid flowing through them. In similar experiments, Levec and Carbonell [7] measured the fluid temperature and solid temperature separately with a series of specially designed probes. The

† Author to whom all correspondence should be sent.

## NOMENCLATURE

| | |
|---|---|
| $a$ | fraction of tubes with $r_1$ in the binary bundle |
| $a_s$ | specific surface area |
| $c$ | specific heat of the medium as a continuum |
| $c_f$ | specific heat of the fluid phase |
| $c_s$ | specific heat of the solid phase |
| $f(r)$ | density distribution function of tube radius of a bundle |
| $G$ | function defined in equation (37) |
| $n$ | ratio of radii, $r_2/r_1$ |
| $P$ | pressure |
| $P_{ed}$ | Peclet number based on Darcy velocity, $2v_d r_w/\alpha_f$ |
| $q_b$ | total heat flux through a bundle |
| $q_i$ | heat flux through the $i$th capillary tube |
| $q_w$ | heat flux through the inner wall of the tube |
| $r$ | coordinate in the radial direction |
| $r_o$ | radius of the outer wall of the tube model |
| $r_w$ | radius of the inner wall of the tube model |
| $S_b$ | cross-sectional area of a bundle |
| $S_i$ | cross-sectional area of the $i$th capillary tube |
| $T$ | temperature of the medium as a continuum |
| $T_f$ | temperature of the fluid phase |
| $T_s$ | temperature of the solid phase |
| $\bar{T}_f$ | average temperature of the fluid phase |
| $\bar{T}_s$ | average temperature of the solid phase |
| $T_w$ | temperature along the inner wall of the tube |
| $t$ | variable of time |
| $V$ | average interstitial velocity of the fluid phase |
| $v(r)$ | dimensionless fluid velocity |
| $v_d$, $\mathbf{v}_d$ | Darcy velocity |
| $v_f(r)$ | actual velocity in the fluid region |
| $z$ | coordinate in the axial direction. |

Greek symbols

| | |
|---|---|
| $\alpha_f$, $\alpha_s$ | thermal diffusivity of the fluid or solid phase |
| $\beta$ | dimensionless number, see equation (32) |
| $\varepsilon$ | small quantity defined by equation (21) |
| $\lambda_d$ | thermal dispersion coefficient |
| $\lambda_e$ | effective thermal conductivity |
| $\lambda_f$ | thermal conductivity of the fluid phase |
| $\lambda_{nd}$ | dimensionless thermal dispersion coefficient |
| $\lambda_s$ | thermal conductivity of the solid phase |
| $\xi$ | coefficient of the bundle |
| $\rho_f$ | density of the fluid phase |
| $\rho_s$ | density of the solid phase |
| $\phi$ | porosity |
| $\Phi$ | function of porosity defined by equation (28). |

data obtained showed that when a temperature front passed through the bed, the profile of the average temperature of the fluid and that of the average temperature of the solid moved at the same speed. The temperature data for each phase was compared to a theoretical model in which the temperature at any point in the fluid region or solid region was decomposed into an average temperature and a local deviation. Good agreement was obtained between the experimental data and the theoretical model.

Other theoretical work has been presented by Dixon and Cresswell [8, 9], Carbonell [10], and Zanotti and Carbonell [11–13]. Dixon and Cresswell [8, 9], by using a two-phase continuum model with a discretized temperature field in the radial direction and perturbation methods, developed approximate expressions predicting the effective axial and radial thermal conductivities and the apparent wall heat transfer coefficient for fluid flow through packed beds in heated tubes. Carbonell [10] introduced the concept of a bundle of capillary tubes of variable diameters to explain molecular dispersion in heterogeneous porous media. Zanotti and Carbonell [13], by using the method of moments and volume averaging, were able to define the thermal dispersion coefficient, expressed in terms of heat capacities, flow rate, thermal conductivities, and porosity for the case of a pulse change in temperature. However, no theoretical model has been reported from which the effective thermal conductivities obtained are directly related to the thermal dispersion coefficient found in equation (1).

In the present work, we start with the energy equations for the fluid region and for the solid region for a single tube model, in order to derive a general equation to express the thermal dispersion coefficient in a form which applies directly to equation (1). The general expression is then applied to two typical cases to generate corresponding coefficients for each case. The two cases are laminar flow with a steady-state temperature distribution and a step-change transient temperature distribution. The effects of heterogeneities on thermal dispersion are examined through the analysis of a bundle of tubes of various radii. Finally the theoretical expressions are compared to the experimental data taken from the literature.

## 2. THERMAL DISPERSION COEFFICIENT FOR A CYLINDRICAL TUBE

The ideal method to deal with the problems of thermal transport in porous media is to separate the

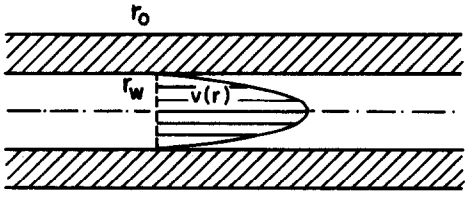


FIG. 1. The thick-walled tube model with fully developed laminar flow inside and insulated condition outside.

problem into a fluid region and a solid region. Closure of the problem is obtained with the appropriate conditions at the interface of the two regions. The geometric complexities of the interface of real porous material exclude this method from practical applications. However, for cases with simple geometry, this method does apply and gives useful and general results.

Consider a long circular tube (Fig. 1) within which fully developed laminar flow occurs. The outer surface of the tube is thermally insulated. The energy equations for this tube–fluid system are

$$\frac{1}{r}\frac{\partial}{\partial r}\left(r\frac{\partial T_f}{\partial r}\right)+\frac{\partial^2 T_f}{\partial x^2}-v_f(r)\frac{1}{\alpha_f}\frac{\partial T_f}{\partial x}=\frac{1}{\alpha_f}\frac{\partial T_f}{\partial t},\quad 0<r<r_w \tag{2}$$

and

$$\frac{1}{r}\frac{\partial}{\partial r}\left(r\frac{\partial T_s}{\partial r}\right)+\frac{\partial^2 T_s}{\partial x^2}=\frac{1}{\alpha_s}\frac{\partial T_s}{\partial t},\quad r_w<r<r_o. \tag{3}$$

At the inner wall of the tube, there are two constraints

$$T_f(x,r_w,t)=T_s(x,r_w,t) \tag{4}$$

and

$$\lambda_f\frac{\partial T_f(x,r_w,t)}{\partial r}=\lambda_s\frac{\partial T_s(x,r_w,t)}{\partial r}. \tag{5}$$

An adiabatic boundary condition is applied at the outer wall of the tube

$$\frac{\partial T_s(x,r_o,t)}{\partial r}=0. \tag{6}$$

By symmetry, at the centerline of the tube

$$\frac{\partial T_f(x,0,t)}{\partial r}=0. \tag{7}$$

The fully developed velocity profile for laminar flow can be expressed as $v_f(r)=2V[1-(r/r_w)^2]$, where $V$ is the average velocity of the fluid inside the tube.

Multiplying equations (2) and (3) by $2\pi r$, integrating with respect to $r$ from 0 to $r_w$ and from $r_w$ to $r_o$, respectively, and then adding the two resultant equations while invoking equations (4)–(7), we have

$$\frac{\partial^2}{\partial x^2}[\lambda_f\phi\bar{T}_f+\lambda_s(1-\phi)\bar{T}_s]-\frac{\rho_f c_f v_d}{\phi}\frac{\partial}{\partial x}\int_0^{r_w}v(r)T_f\,d\left(\frac{r}{r_o}\right)^2=\frac{\partial}{\partial t}[\rho_f c_f\phi\bar{T}_f+\rho_s c_s(1-\phi)\bar{T}_s] \tag{8}$$

where $v(r)=2[1-(r/r_w)^2]$, while $\bar{T}_f$ and $\bar{T}_s$ are the average temperature of fluid phase and solid phase, respectively, defined as

$$\bar{T}_f\equiv\frac{\int_0^{r_w}T_f\,d(r^2)}{r_w^2} \tag{9}$$

and

$$\bar{T}_s\equiv\frac{\int_{r_w}^{r_o}T_s\,d(r^2)}{r_o^2-r_w^2}. \tag{10}$$

In this particular tube model, porosity $\phi=r_w^2/r_o^2$.

If a tube with a large aspect ratio (i.e. $L/r_o\gg 1$) is considered as a one-dimensional continuum, equation (1) becomes

$$\frac{\partial}{\partial x}\left(\lambda_d\frac{\partial T}{\partial x}\right)-\rho_f c_f v_d\frac{\partial T}{\partial x}=[\rho_f c_f\phi+\rho_s c_s(1-\phi)]\frac{\partial T}{\partial t} \tag{11}$$

where $T$ is the average temperature obtained over a cross-sectional area. The average temperature $T$ is defined as

$$T\equiv\frac{\rho_f c_f\phi\bar{T}_f+\rho_s c_s(1-\phi)\bar{T}_s}{\rho_f c_f\phi+\rho_s c_s(1-\phi)}. \tag{12}$$

Subtracting equation (8) from equation (11), we have

$$\frac{\partial}{\partial x}\left[\lambda_d\frac{\partial T}{\partial x}-\lambda_f\phi\frac{\partial\bar{T}_f}{\partial x}-\lambda_s(1-\phi)\frac{\partial\bar{T}_s}{\partial x}-\rho_f c_f v_d\left[T-\frac{1}{\phi}\int_0^{r_w}v(r)T_f\,d\left(\frac{r^2}{r_o^2}\right)\right]\right]=0.$$

In general, the bracketed term is a function of time. The spatial integration of the above equation leads to the following:

$$\lambda_d\frac{\partial T}{\partial x}-\lambda_f\phi\frac{\partial\bar{T}_f}{\partial x}-\lambda_s(1-\phi)\frac{\partial\bar{T}_s}{\partial x}-\rho_f c_f v_d\left[T-\frac{1}{\phi}\int_0^{r_w}v(r)T_f\,d\left(\frac{r^2}{r_o^2}\right)\right]=H(t).$$

Physically the term $H(t)$ represents the discrepancy in the heat flux of the one- and two-equation models. However, we require the heat flux through the two models to be the same. Thus, we set $H(t)=0$ and then solve for the thermal dispersion coefficient $\lambda_d$ as

$$\lambda_d = \left\{\lambda_f \int_0^{r_w} \frac{\partial T_f}{\partial x} d\left(\frac{r}{r_o}\right)^2 + \lambda_s \int_{r_w}^{r_o} \frac{\partial T_s}{\partial x} d\left(\frac{r}{r_o}\right)^2 + \rho_f c_f v_d \left[T - \frac{1}{\phi}\int_0^{r_w} v(r) T_f d\left(\frac{r}{r_o}\right)^2\right]\right\}\left(\frac{dT}{dx}\right)^{-1}. \quad (13)$$

It can be seen that once the functions $T_f(x, r, t)$ and $T_s(x, r, t)$ in equations (2) and (3) are given, we may substitute them into equations (9), (10), (12) and (13), and obtain $\lambda_d$ as a function of $x$ and $t$. Therefore, for each particular temperature distribution satisfying equations (2) and (3), there exists a corresponding thermal dispersion coefficient function which can be used in equation (11). When a set of boundary conditions in the $x$-direction is imposed, equations (2) and (3), subject to conditions (4)–(7), form a closed problem which may be solved by analytical or numerical methods. The dispersion coefficient $\lambda_d$ can then be obtained by use of equation (13). Equation (13) is valid under both steady-state and transient conditions since the transient terms of equations (2) and (3) have not been dropped.

Equation (13) indicates that the thermal dispersion coefficient depends not only on the physical properties of the fluid phase and the solid phase, but also on the velocity field and the temperature field in these two phases. Therefore, we should not expect to find a single expression for $\lambda_d$ which applies to all flow regimes and temperature distributions. However, for each particular case, there should be a corresponding solution for $\lambda_d$.

## 3. ASYMPTOTIC SOLUTIONS OF TWO CASES

Our major concern in this work is the interior region of the porous medium. Here we assume that the primary mechanism of thermal dispersion is enhanced pore-level convection due to the existence of an interstitial velocity profile. Therefore, we proceed with a specified pore-level velocity profile and examine variations in the overall temperature field under given thermal boundary conditions. The flow inside the pores is considered to be fully developed. For the laminar flow regime, the velocity profile is then parabolic. The temperature distribution evolves from either the steady-state or unsteady-state condition. A packed bed with a heat source at one end and heat sink at the other is an example of a steady-state problem. A number of unsteady-state problems often encountered in real applications can be referred to as traveling front problems in which there exists a step change in the inlet temperature of the flowing fluid. As the fluid passes through the medium, the temperature front smears out along the flow direction because of the combined effects of molecular diffusion and hydraulic dispersion. Thus, the two typical cases of interest are: laminar flow with steady-state temperature distribution and laminar flow with traveling-front temperature distribution. In what follows, we will derive the asymptotic solutions for these two cases where the aspect ratio of the tube is large.

### 3.1. *Laminar flow with steady-state temperature distribution*

In most applications, the dimensions of the region of interest are much larger than those of the pores or grains of the medium so that a tube model with a large aspect ratio can be used to simulate the medium. We are interested in thermal dispersion in the interior region where the end effects resulting from the imposed conditions of uniform temperatures at both ends are not important. Equations (2) and (3), subject to equations (4)–(7) with the additional isothermal conditions at two ends, were first solved by numerical methods. The numerical solutions indicate that when the aspect ratio of the tube is large, the temperature distributions in the fluid and solid are linear in the $x$-direction in the middle portion of the tube, i.e.

$$\frac{\partial T_f}{\partial x} = \frac{\partial T_s}{\partial x} = \frac{\partial T}{\partial x}. \quad (14)$$

Substituting equation (14) and the parabolic velocity profile into equation (13) yields

$$\lambda_d = \phi\lambda_f + (1-\phi)\lambda_s + \frac{\rho_f c_f v_d \left\{T - \frac{2}{\phi}\int_0^{r_w}\left[1-\left(\frac{r}{r_o}\right)^2\right] T_f d\left(\frac{r}{r_o}\right)^2\right\}}{\frac{dT}{dx}}. \quad (15)$$

It can be seen that the first two terms on the right-hand side of equation (15) are exactly equal to the static effective thermal conductivity of the tube–fluid system which can be viewed as an example of a parallel model of porous media. The third term of equation (15) is the dispersive contribution of the pore level fluid velocity distribution. Denoting the static conductivity by $\lambda_e$, i.e.

$$\lambda_e = \phi\lambda_f + (1-\phi)\lambda_s \quad (16)$$

and defining the Peclet number, $P_{ed}$, in the following manner

$$P_{ed} = \frac{2r_w v_d}{\alpha_f} \quad (17)$$

the dimensionless thermal dispersion coefficient $\lambda_{nd}$, defined as $\lambda_d/\lambda_e$, can be expressed as

$$\lambda_{nd} = 1 + \frac{\frac{P_{ed}\lambda_f}{r_w\lambda_e}\left\{\frac{T}{2} - \frac{1}{\phi}\int_0^{r_w}\left[1-\left(\frac{r}{r_w}\right)^2\right] T_f d\left(\frac{r}{r_o}\right)^2\right\}}{\frac{dT}{dx}}. \quad (18)$$

The second term on the right-hand side of equation

(18) indicates the relative increase in the thermal conductance due to the fluid velocity variations.

In order to use equation (18), $T_f$, $T_s$ and $T$ from equations (3) and (4) are needed under the condition of a large aspect ratio. For steady state, equation (3) becomes

$$\frac{1}{r}\frac{\partial}{\partial r}\left(r\frac{\partial T_s}{\partial r}\right)+\frac{\partial^2 T_s}{\partial x^2}=0. \tag{19}$$

Multiplying equation (19) by $2\pi r$ and then integrating with respect to $r$ from $r_w$ to $r_o$ and invoking the adiabatic boundary condition at $r_o$, we have

$$\frac{d^2\bar{T}_s}{dx^2}=-\frac{2q_w\sqrt{\phi}}{\lambda_s r_o(1-\phi)} \tag{20}$$

where $\bar{T}_s$ is the average temperature of the solid region defined by equation (10) and $q_w$ the local heat flux from the fluid region through the inner wall of the tube into the solid region. Here $q_w$ is positive when the heat flux is in the positive $r$-direction. In general, both $\bar{T}_s$ and $q_w$ are functions of $x$. Since the outer wall of the tube is considered to be adiabatic, the only cause of heat flow is the heat source and heat sink at the two ends of the tube. Thus, when the aspect ratio of the tube is large, the heat flux through the inner wall must be small. As an approximation, let us assume that $q_w$ has a small constant value. Denoting the right-hand side of equation (20) by $-\varepsilon$, i.e.

$$\varepsilon=\frac{2q_w\sqrt{\phi}}{\lambda_s r_o(1-\phi)} \tag{21}$$

we may rewrite equation (20) as

$$\frac{d^2\bar{T}_s}{dx^2}=-\varepsilon. \tag{22}$$

Since in the middle portion of the tube, $\partial T_s/\partial x$ is independent of $r$, we may further assume

$$\frac{\partial^2 T_s}{\partial x^2}\approx\frac{d^2\bar{T}_s}{dx^2}=-\varepsilon. \tag{23}$$

Substituting equation (23) into equation (19) yields

$$\frac{1}{r}\frac{\partial}{\partial r}\left(r\frac{\partial T_s}{\partial r}\right)=\varepsilon. \tag{24}$$

Integrating equation (24) twice with respect to $r$ and invoking the boundary conditions

$$\left(\frac{\partial T_s}{\partial r}\right)_{r_o=0}=0$$

and

$$-\lambda_s\left(\frac{\partial T_s}{\partial r}\right)_{r=r_w}=q_w$$

we have

$$T_s(x,r)=T_w(x)+\frac{q_w r_o}{2\lambda_s}\left(\frac{\sqrt{\phi}}{1-\phi}\right)\left[\frac{(r^2-r_w^2)}{r_o^2}-\ln\left(\frac{r}{r_w}\right)^2\right]. \tag{25}$$

Since the heat flux at the wall $q_w$ is assumed to be constant, the well-known solution [14] for laminar flow in a tube with fully developed temperature profile and constant heat flux at the wall applies to the fluid region inside the tube, i.e.

$$T_f(x,r)=T_w(x)+\frac{q_w r_w}{4\lambda_f}\left[\left(\frac{r}{r_w}\right)^4-4\left(\frac{r}{r_w}\right)^2+3\right]. \tag{26}$$

Substituting equations (25) and (26) into equations (9) and (10) and then substituting the resultant $\bar{T}_f$ and $\bar{T}_s$ into equation (12), we find

$$T=T_w(x)+\frac{q_w r_o\sqrt{\phi}}{\lambda_s}\left[\frac{\rho_f c_f\phi\left(\frac{\lambda_s}{3\lambda_f}\right)-\frac{\rho_s c_s\Phi}{4(1-\phi)}}{\rho_f c_f\phi+\rho_s c_s(1-\phi)}\right] \tag{27}$$

where

$$\Phi=4\phi-3-\phi^2-\ln\phi^2. \tag{28}$$

The dimensionless thermal dispersion coefficient $\lambda_{nd}$ can be obtained from equations (18), (27) and (26)

$$\lambda_{nd}=1+\left(\frac{P_{ed}q_w}{6\lambda_e}\right)\times\left[\frac{\rho_f c_f\phi-\frac{3\rho_s c_s\Phi}{4(1-\phi)}\left(\frac{\lambda_f}{\lambda_s}\right)}{\rho_f c_f\phi+\rho_s c_s(1-\phi)}-\frac{11}{8}\right]\left(\frac{dT_w}{dx}\right)^{-1}. \tag{29}$$

Based on an energy balance in the fluid region, the heat flux across the wall can be related to the gradient of the average fluid temperature

$$q_w=-\frac{P_{ed}\lambda_f}{4\phi}\frac{d\bar{T}_f}{dx}. \tag{30}$$

It is now obvious that the assumptions of equation (14) also result in

$$\frac{dT}{dx}=\frac{d\bar{T}_f}{dx}=\frac{dT_w}{dx}. \tag{31}$$

Substituting equations (30) and (31) into equation (29) then yields

$$\lambda_{nd}=1+\frac{P_{ed}^2}{24\phi}\left(\frac{\lambda_f}{\lambda_e}\right)\left\{\frac{3}{8}+\frac{\beta\left[(1-\phi)+\frac{3\Phi}{4(1-\phi)}\left(\frac{\lambda_f}{\lambda_s}\right)\right]}{\phi+\beta(1-\phi)}\right\} \tag{32}$$

where

$$\beta=\frac{\rho_s c_s}{\rho_f c_f}.$$

It is encouraging to note that neither the solid–fluid

heat flux $q_w$ nor the temperature gradient appears in equation (32). Also, the thermal dispersion is now seen to be defined only by the physical properties of the solid and fluid phases, the porosity of the tube/fluid system and the flow rate, expressed in a dimensionless fashion as the Peclet number.

### 3.2. *Laminar flow with traveling front temperature distribution*

Since in equations (2) and (11) there exist both diffusion and convection terms, a sharp temperature front in the flowing fluid would be expected to spread out in the flow direction while moving downstream. It is obvious that the solution of the problem can be simplified with a moving coordinate system at the average velocity of the temperature front. The velocity of the moving front, $v_c$, is defined as

$$v_c = \frac{\rho_f c_f v_d}{\rho_f c_f \phi + \rho_s c_s (1-\phi)}. \tag{33}$$

Upon transformation from the $x$–$t$ plane to the $x_1$–$t_1$ plane, where $x_1 = x - v_c t$ and $t_1 = t$, equation (11) becomes

$$\lambda_d \frac{\partial^2 T}{\partial x_1^2} = [\rho_f c_f \phi + \rho_s c_s (1-\phi)] \frac{\partial T}{\partial t_1}. \tag{34}$$

It is well known that equation (34) has a similarity solution of error function form when subjected to the boundary conditions of two constant temperatures, at $-\infty$ and at $+\infty$, and the initial condition of a step function. The initial step function will spread out symmetrically with respect to the origin of the moving coordinate. Therefore, $v_c$ can be referred to as the characteristic velocity of the moving front. It is interesting to note that this characteristic velocity $v_c$ is identical to the velocities for the fronts of the average solid temperature and the average fluid phase temperature, as obtained by Zanotti and Carbonell [12] using the moment method for a pulse increase in temperature.

Transforming equations (2) and (3) to the moving coordinate system and, following a similar procedure used in deriving equation (18), we find that the dimensionless thermal dispersion coefficient $\lambda_{nd}$ becomes

$$\lambda_{nd} = 1 + \frac{P_{ed}\lambda_f}{2\lambda_e[\phi + \beta(1-\phi)]} \left\{ \int_{r_w}^{r_o} \beta T_s \, d\left(\frac{r}{r_o}\right)^2 - \int_0^{r_w} \left[\frac{v_f(r)}{v_c} - 1\right] T_f \, d\left(\frac{r}{r_o}\right)^2 \right\} \left(\frac{dT}{dx}\right)^{-1}. \tag{35}$$

For long times, the temperature front will have a certain width in $x$ instead of a sharp front. If the width is large enough in comparison with the radius of the tube, we may employ the approximation that the fluid temperature is linear with respect to $x_1$. We may also assume that the heat flux across the inner wall of the tube is a small constant value in the front region. In contrast to the assumption of a negligible axial derivative of the liquid temperature deviation used by Zanotti and Carbonell [13], we assume that all axial temperature derivatives are equal. Following the same procedure as in the steady-state case, we may find the temperature distributions in both the solid and fluid regions. Substituting these temperature profiles into equation (35), we finally obtain the following expression for $\lambda_{nd}$:

$$\lambda_{nd} = 1 + \frac{P_{cd}^2}{192\phi}\left(\frac{\lambda_f}{\lambda_e}\right) \times \frac{\left[\phi^2 + 6\beta\phi(1-\phi) + 11\beta^2(1-\phi^2) + 6\left(\frac{\lambda_f}{\lambda_s}\right)\beta^2\Phi\right]}{[\phi + \beta(1-\phi)]^2} \tag{36}$$

If the porosity is unity, the wall of the tube does not play a role in the heat transfer process and equation (36) gives the well-known Taylor–Aris expression [15] for the species dispersion coefficient, as expected.

It is of note that in both equations (32) and (36), the dimensionless dispersion coefficient $\lambda_{nd}$ is never less than one. In these two equations, the parameter $\Phi$ defined by equation (28) is always positive if the porosity varies from zero to one. Therefore, the flow in a porous medium always increases the dispersive heat transfer when such flow is parallel to the heat flux direction under either co-current or counter-current conditions.

## 4. EFFECTS OF HETEROGENEITIES

Heterogeneity is an inherent feature of all real porous media. From a conceptual standpoint, it is obvious that preferential fluid flow through a larger diameter 'tube' will enhance thermal dispersion in heterogeneous media due to the mechanisms identified in previous sections. Thus, an investigation of the effects of heterogeneities on thermal dispersion in porous media is particularly valuable.

A bundle of tubes, with $f(r_w)$ being the distribution function of the radii of the inner walls of the tubes, is employed as the simplest model of heterogeneous porous media. Assuming that each tube in the bundle has the same ratio of the radius of the outer wall to that of the inner wall, all tubes in the bundle, as well as the whole bundle, have the same porosity, i.e. $\phi_i = (r_{wi}/r_{oi})^2 = \phi_b$, where the subscript $i$ indicates quantities of the $i$th tube in the bundle, and subscript b indicates those quantities for the whole bundle. If both the liquid phase and the solid phase have uniform properties, $\lambda_s/\lambda_f$ and $\beta$ are constant throughout the bundle. Assume further that the whole bundle is sufficiently long so that each tube in the bundle has a large aspect ratio and that the temperature gradients

in the axial direction of each tube are identical to that of the whole bundle. Normally the thermal conductivity of the solid phase is much higher than that of the liquid phase so that the temperature varies almost linearly along the entire outer wall of the tube, including the regions next to the two ends. Therefore, it is reasonable to assume that at each cross-sectional area, the temperatures at the outer walls of the tubes are identical so that there is no heat exchange taking place between tubes. An adiabatic boundary condition can then be imposed at the outer wall of each tube. Thus, each tube in the bundle is under exactly the same situation as the previous single tube model and equations (32) and (36) apply. It is convenient to write both equations (32) and (36) in the form of

$$\lambda_{nd} = 1 + P_{ed}^2 G\left(\phi, \frac{\lambda_s}{\lambda_f}, \beta\right) \tag{37}$$

where function $G$ is defined either by equation (32) or (36), depending on the situation. In both cases $G$ is only a function of porosity, the conductivity ratio of the two phases, and the specific heats of the two phases so that it is a constant for the bundle, i.e. $G_i \equiv G_b$.

The dispersive heat flux of the $i$th tube is

$$q_i = -\lambda_{di}\frac{dT_i}{dx} \tag{38}$$

where $T_i$ is the average temperature over a cross-sectional area of the $i$th tube and $\lambda_{di}$ the thermal dispersion coefficient of the $i$th tube, as given by equation (32) or (36). By definition, the dispersive heat flux of the whole bundle is

$$q_b = -\lambda_{db}\frac{dT_b}{dx} \tag{39}$$

where $T_b$ is the average temperature of the bundle over any whole cross-sectional area and $\lambda_{db}$ the thermal dispersion coefficient for the whole bundle. Since the temperature gradients in the $x$-direction are constant

$$\frac{dT_i}{dx} = \frac{dT_b}{dx}. \tag{40}$$

The heat flux of the bundle must equal the total heat flow divided by the total area of the bundle, thus

$$q_b = \frac{\Sigma q_i S_i}{\Sigma S_i} \tag{41}$$

where $S_i$ is the total cross-sectional area of the $i$th tube.

Substituting equations (38) and (39) into equation (41), we obtain

$$\lambda_{db} = \frac{\Sigma \lambda_{di} S_i}{\Sigma S_i}. \tag{42}$$

Assuming Poiseuille flow in tubes and that the pressure gradients are constant, for the $i$th tube we have

$$v_{di} = \phi\frac{r_{wi}^2}{8\mu}\frac{dP}{dx}. \tag{43}$$

The overall Darcy velocity of the whole bundle can be expressed as

$$v_{db} = \frac{\int_0^\infty r_w^4 f(r_w)\,dr_w}{\int_0^\infty r_w^2 f(r_w)\,dr_w}\left(\frac{\phi}{8\mu}\frac{dP}{dx}\right) \tag{44}$$

and the Peclet number, $P_{edb}$, based on the Darcy velocity of the whole bundle, $v_{db}$, and the average radius of the bundle, $\bar{r}_w$, is then

$$P_{edb} = \frac{\int_0^\infty r_w^4 f(r_w)\,dr_w}{\int_0^\infty r_w^2 f(r_w)\,dr_w}\left(\frac{\bar{r}_w\phi}{4\alpha_f\mu}\frac{dP}{dx}\right). \tag{45}$$

Since the porosity and the thermal conductivities of the fluid phase and the solid phase of all the tubes in the bundle are identical, the static thermal conductivity of the bundle must be identical to that of any one of the tubes. Denoting the static thermal conductivity of a single tube and of the whole bundle as $\lambda_e$, dividing both sides of equation (42) by $\lambda_e$, and converting from a discrete form to a continuous form, we have

$$\lambda_{ndb} = \frac{\int_0^\infty \lambda_{nd} r_w^2 f(r_w)\,dr_w}{\int_0^\infty r_w^2 f(r_w)\,dr_w} \tag{46}$$

where $\lambda_{ndb}$ is the dimensionless thermal dispersion coefficient of the whole bundle. By substituting equations (36) and (45) into equation (46), the following is obtained:

$$\lambda_{ndb} = 1 + P_{edb}^2 G\left(\phi, \frac{\lambda_s}{\lambda_f}, \beta\right)\xi \tag{47}$$

where the coefficient $\xi$ is defined by

$$\xi = \frac{\int_0^\infty r_w^8 f(r_w)\,dr_w \cdot \int_0^\infty r_w^2 f(r_w)\,dr_w}{\bar{r}_w^2\left[\int_0^\infty r_w^4 f(r_w)\,dr_w\right]^2}. \tag{48}$$

Note that $\xi$ is only a function of the tube size distribution function $f(r_w)$ of the bundle. Comparison of equation (47) with equation (37) shows that the dimensionless thermal dispersion coefficient of a bundle equals that of a tube of average radius with the second term multiplied by $\xi$. Therefore, as long as the radius distribution function, $f(r)$, of a bundle is known, the dispersion coefficient for the bundle can be evaluated from equations (47) and (48).

Equation (47) shows that the effect of heterogeneities on the thermal dispersion coefficient depends on the function $\xi$. A homogeneous medium can be viewed as a particular case of a heterogeneous medium

with radius distribution function being defined by a Dirac delta function, i.e. $f(r_w) = \delta(r_{wo})$. This uniform distribution gives $\xi = 1$ for a homogeneous medium as it should. The values of $\xi$ corresponding to some well-known distribution functions are given in Table 1. By the wide range of $\xi$ values illustrated in Table 1, it is clear that heterogeneities can be a dominant factor in dispersive heat transfer.

To gain a better understanding of the behavior of the function $\xi$, we examine a binary system consisting of only two sizes of tubes with radii being $r_1$ and $r_2$. The distribution function of the system is

$$f(r) = a\delta(r_1) + (1-a)\delta(r_2) \tag{49}$$

where $a$ is the fraction of tubes of $r_1$, and $0 \leqslant a \leqslant 1$. Denoting the ratio $r_2/r_1$ by $n$ and substituting equation (49) into equation (48), the function $\xi$ of the binary system becomes

$$\xi = \frac{[a+(1-a)n^8]\cdot[a+(1-a)n^2]}{[a+(1-a)n]^2\cdot[a+(1-a)n^4]^2}. \tag{50}$$

From equation (50) we see that when $a = 0$, $a = 1$, or $n = 1$, $\xi = 1$ which is consistent with the case of homogeneous media. Equation (50) is illustrated in Fig. 2 for several values of $n \geqslant 1$. In Fig. 2, $\xi$ increases with the ratio of tube radii, $n$, until it reaches a maximum value, then decreases rapidly to a value of one at $a = 1$. The larger the value of $n$, the higher the value of $\xi$. Thus thermal dispersion will be much more pronounced if there are a few larger channels in a uniform medium with relatively small pores, than if no channels are present. The other interesting feature of the binary system is that when the percentage of the large tubes is very small, i.e. when $a \to 1$, $\xi$ changes dramatically to a value of 1.0. Therefore, thermal dispersion coefficients are somewhat unpredictable in a real porous medium because it is very difficult to evaluate the exact percentage and sizes of the larger pores.

## 5. COMPARISON OF THEORY WITH EXPERIMENTAL RESULTS

The predictions from equations (32) and (36) may be compared with published data where available. Inevitably, the errors in such data stemming from the assumptions made in data reduction and other uncertainties such as uneven packing, natural cracks, etc., result in low accuracy of the thermal dispersion coefficients. Therefore, we can expect qualitative comparison rather than precise matches between the theoretical results and the experimental data. For purposes of comparison, the Peclet number in equations (32) and (36), which is based on the radius of the tube, is converted to the Peclet number based on particle diameter for the same specific surface area. The specific surface area of a packed bed can be expressed in terms of the mean particle diameter and the porosity [13]

$$a_s = \frac{6(1-\phi)}{d_p}.$$

For the tube model

$$a_s = \frac{2\phi}{r_w}.$$

Therefore, the particle diameter can be related to the radius of the tube as follows:

$$d_p = 3\left(\frac{1}{\phi} - 1\right) r_w.$$

Figures 3–6 show the results obtained by Yagi *et al.* (1960) [1], Gunn and De Souza (1974) [6] and Green *et al.* (1964) [5] from various transient flow experiments. Figure 7 shows the most recent results obtained by Levec and Carbonell (1985) [7] from their experiments of the transient process with specially designed temperature probes. The solid lines on Figs. 3–7 are the predictions from use of equation (36) whereas the dashed lines in Figs. 3–6 are the predictions from Zanotti and Carbonell's model [13]. The dashed lines in Fig. 7 are from Levec and Carbonell's theory [7, 16]. In most cases, the experimental data are rather scattered. However, the predictions based on equation (36) are generally in good agreement with these data in the region of Peclet number up to 100, except in Fig. 6 where the experimental data are higher than the calculated values. When the Peclet number exceeds 100, the predictions from equation (36) tend to be higher than experimental results, presumably because of the change in flow regime. In the transitional and turbulent regimes of higher Reynolds number flows, the velocity profile would not be parabolic and downstream recirculation or the turbulence of the fluid may provide an increased cross-stream transport, which would decrease the dispersive mechanisms included in this analysis. Thus, the linear dependency of the thermal dispersion coefficient on the Peclet number observed at high flow rates is not surprising.

Results of steady-state experiments conducted by Kunii and Smith (1961) [2] are shown on Fig. 8 where experimental data are cast into dimensionless conductivity vs Peclet number. For purposes of comparison, a least square regression method was applied to the experimental data to obtain a best-fit correlation between conductivities and Peclet number. This correlation was extrapolated to zero Peclet number to determine the static conductivity which is, in turn, used to normalize the experimental data as plotted on Fig. 8. Since the Peclet numbers in Fig. 8 are very low, the dominant part of the coefficient is the static conductivity. The contribution of the fluid flow to the coefficient is very small, as supported by the fact that the data of dimensionless conductivity fall in a narrow range around one. The solid line in Fig. 8 shows the dimensionless conductivity predicted by equation (32). The experimental data appear to increase with respect to the Peclet number at a rate somewhat higher than those predicted by equation (32). However, this

Table 1. Values of $\xi$ for certain distribution functions

| Name | Function | Mean | Plot | $\xi$ |
|---|---|---|---|---|
| Gamma<br>$\Gamma(\alpha, \beta)$ | $f_\Gamma(r) = \begin{cases} \frac{\beta^\alpha}{\Gamma(\alpha)} r^{\alpha-1} e^{-\beta r} & r > 0 \\ 0 & r \leqslant 0 \end{cases}$ | $\frac{\alpha}{\beta}$ | 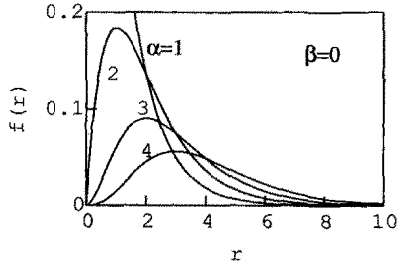 | $\frac{(\alpha+4)\cdots(\alpha+7)}{\alpha^2(\alpha+2)(\alpha+3)}$<br>α ξ<br>1 140<br>2 37.8<br>3 10.0 |
| Logarithm normal<br>$L_n(\mu, \sigma^2)$ | $f_{L_n}(r) = \begin{cases} \frac{1}{\sqrt{(2\pi)}\sigma r} e^{-(\ln r-\mu)^2/2\sigma^2} & r > 0 \\ 0 & r \leqslant 0 \end{cases}$ | $e^{\mu+(\sigma^2/2)}$ | 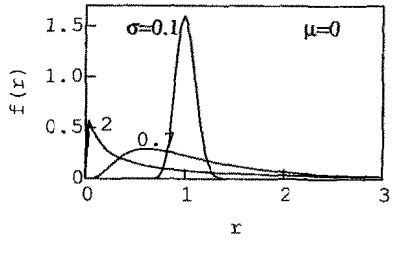 | $e^{1.7\sigma^2}$<br>σ ξ<br>0.1 1.2<br>2.0 4.6<br>3.0 $4.1 \times 10^3$ |
| Weber<br>$W(m, \alpha)$ | $f_W(r) = \begin{cases} \frac{m}{\alpha} r^{m-1} e^{-r^m/\alpha} & r > 0 \\ 0 & r \leqslant 0 \end{cases}$ | $\alpha^{1/m}\Gamma\left(1+\frac{1}{m}\right)$ | 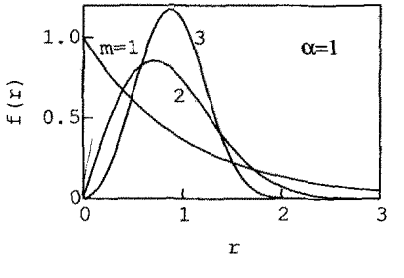 | $\frac{\Gamma\left(\frac{8}{m}+1\right)\Gamma\left(\frac{2}{m}+1\right)}{\Gamma^2\left(\frac{1}{m}+1\right)\Gamma^2\left(\frac{4}{m}+1\right)}$<br>m ξ<br>1 140.0<br>2 7.6 |

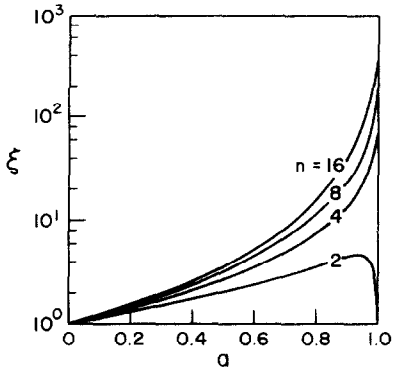


FIG. 2. Correlations between heterogeneity coefficient $\xi$ and fraction of tubes with smaller radius $r_1$ in a binary bundle.

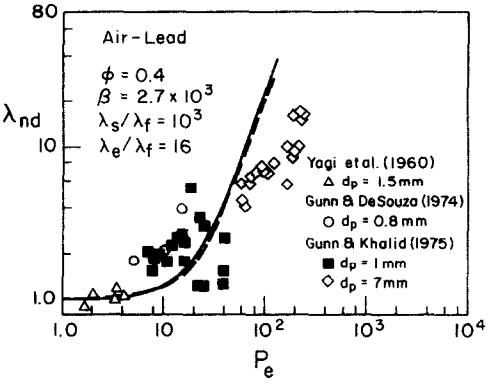


FIG. 5. Dimensionless dispersion coefficient vs Peclet number for transient condition of air–lead system.

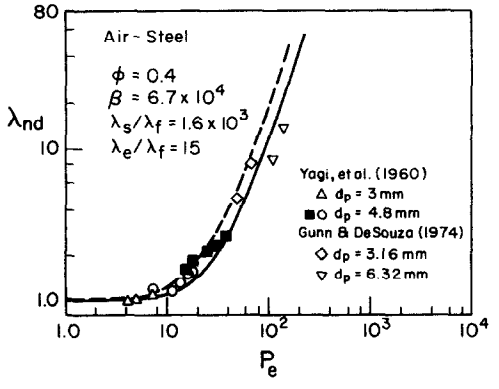


FIG. 3. Dimensionless dispersion coefficient vs Peclet number for transient condition of air–steel system.

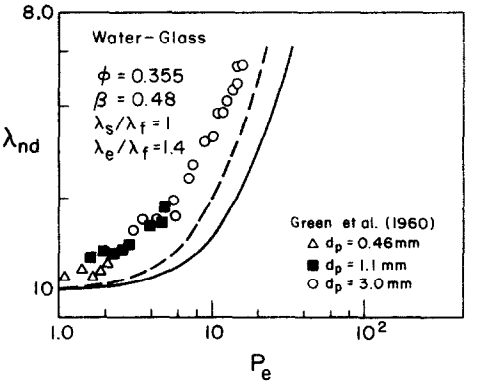


FIG. 6. Dimensionless dispersion coefficient vs Peclet number for transient condition of water–glass system.

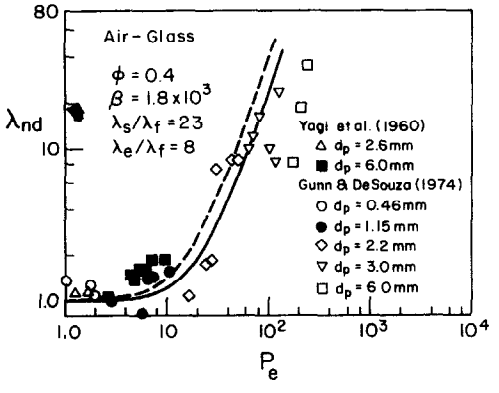


FIG. 4. Dimensionless dispersion coefficient vs Peclet number for transient condition of air–glass system.

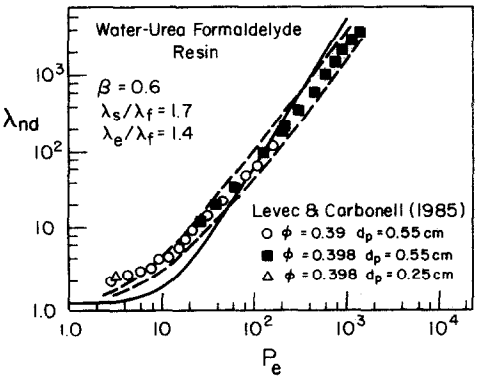


FIG. 7. Dimensionless dispersion coefficient vs Peclet number for transient condition. Temperatures of solid phase and liquid phase were measured separately with special probes.

discrepancy may be due to experimental errors, the simplified model used to reduce the data, and/or the heterogeneity effects.

## 6. CONCLUSIONS

Several conclusions can be drawn from the theoretical analysis presented herein:

(1) The thermal dispersion coefficient for a porous medium with a flowing fluid depends on the velocity field and the temperature field of the system. For a specific flow regime and temperature field, there exists a corresponding relationship between the thermal dispersion coefficient and the Peclet number. Other than integral forms such as equation (13), there is no general definition of a thermal dispersion coefficient for an arbitrary thermal field.

(2) In the laminar flow regime, for which the Peclet number is small ($< 100$), the dispersion coefficient equals the static thermal conductivity plus a term due to the contribution of dispersive flow. This latter term

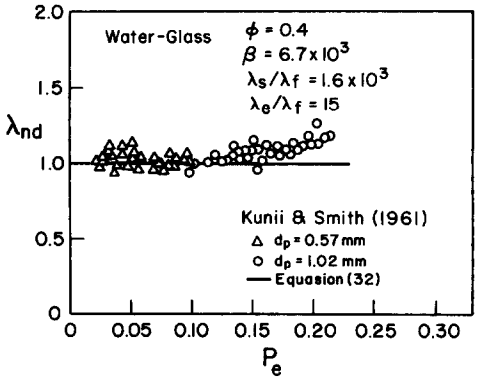


FIG. 8. Dimensionless dispersion coefficient vs Peclet number for steady-state temperature distribution in a range of low Peclet numbers.

is proportional to the Peclet number squared. The proportionality constant is a function of porosity, the ratio of thermal conductivities of two phases, the ratio of the specific heats and densities of the two phases, and the temperature field pattern.

(3) Thermal dispersion resulting from heterogeneities varies over a wide range. Under certain circumstances, heterogeneities are predicted to cause several orders of magnitude increase in the thermal dispersion coefficient.

*Acknowledgement*—This work was performed through funding from Chevron Oil Field Research. The support provided is gratefully acknowledged.

## REFERENCES

1. S. Yagi, D. Kunii and N. Wakao, Studies on axial effective thermal conductivities in packed beds, *A.I.Ch.E. Jl* **6**(4), 543–546 (December 1960).
2. D. Kunii and J. M. Smith, Heat transfer characteristics of porous rocks: II. Thermal conductivities of unconsolidated particles with flowing fluids, *A.I.Ch.E. Jl* **7**(1), 29–34 (March 1961).
3. G. P. Willhite, D. Kunii and J. M. Smith, Heat transfer in beds of fine particles, *A.I.Ch.E. Jl* **8**(3), 340–345 (July 1962).
4. P. Adivarahan, D. Kunii and J. M. Smith, Heat transfer in porous rocks through which single-phase fluids are flowing, *SPEJ* 290–296 (September 1962).
5. D. W. Green, R. H. Perry and R. E. Babcock, Longitudinal dispersion of thermal energy through porous media with a flowing fluid, *A.I.Ch.E. Jl* **10**(5), 645–651 (September 1964).
6. D. J. Gunn and J. F. C. De Souza, Heat transfer and axial dispersion in packed beds, *Chem. Engng Sci.* **29**, 1363–1371 (1974).
7. J. Levec and R. G. Carbonell, Longitudinal and lateral thermal dispersion in packed beds, Part II, *A.I.Ch.E. Jl* **31**(4), 591–602 (April 1985).
8. A. G. Dixon and D. L. Cresswell, Theoretical prediction of effective heat transfer parameters in packed beds, *A.I.Ch.E. Jl* **25**(4), 663–676 (July 1979).
9. D. L. Cresswell and A. G. Dixon, Reply to comments by Vortmeyer and Berninger on the paper "Theoretical prediction of effective heat transfer parameters in packed beds (*A.I.Ch.E. Jl* **25**, 663 (1979))", *A.I.Ch.E. Jl* **28**(3), 511–513 (May 1982).
10. R. G. Carbonell, Effect of pore distribution and flow segregation on dispersion in porous media, *Chem. Engng Sci.* **34**, 1031–1039 (1979).
11. F. Zanotti and R. G. Carbonell, Development of transport equations for multiphase systems—I, *Chem. Engng Sci.* **39**(2), 263–278 (1984).
12. F. Zanotti and R. G. Carbonell, Development of transport equations for multiphase systems—II, *Chem. Engng Sci.* **39**(2), 279–297 (1984).
13. F. Zanotti and R. G. Carbonell, Development of transport equations for multiphase systems—III, *Chem. Engng Sci.* **39**(2), 299–311 (1984).
14. W. M. Crawford and M. E. Kays, *Convective Heat and Mass Transfer*, 2nd Edn, pp. 94–96. McGraw-Hill, New York (1980).
15. R. Aris, On the dispersion of a solute in a fluid flowing through a tube, *Proc. R. Soc.* **A235**, 67 (1956).
16. J. Levec and R. G. Carbonell, Longitudinal and lateral thermal dispersion in packed beds, Part I, *A.I.Ch.E. Jl* **31**(4), 581–590 (April 1985).

## DISPERSION THERMIQUE DANS DES TUBES A PAROI EPAISSE COMME MODELE DES MILIEUX POREUX

**Résumé**—On présente une étude théorique de la dispersion thermique dans les milieux poreux. La contribution des distributions du niveau de vitesse à la dispersion est considérée dans une analyse du transport thermique dans un tube à paroi épaisse contenant un fluide en écoulement. On montre que les cas d'un gradient de température appliqué en permanence et d'une onde progressive de température produisent des dispersions thermique différentes. Dans les deux cas, le coefficient de dispersion est défini par la conductivité thermique statique plus un terme dû à l'écoulement dispersif. Ce terme est proportionnel au carré du nombre de Péclet. Le coefficient de proportionalité est fonction de la porosité, des propriétés thermiques du fluide et du solide, et du champ de température. En considérant une grappe de tubes de différents diamètres, la contribution des hétérogénéités est évaluée. Des variations dans le diamètre des pores causent des accroissements de dispersion de plusieurs ordre de grandeur. Des comparaisons satisfaisantes du modèle de dispersion et des données expérimentales sont présentées.

## THERMISCHE DISPERSION IN DICKWANDIGEN ROHREN ALS MODELL EINES PORÖSEN MEDIUMS

**Zusammenfassung**—Es wird eine theoretische Untersuchung der thermischen Dispersion in porösen Medien vorgestellt. Der Einfluß der Geschwindigkeitsverteilung in der Porenebene auf die Dispersion wird in eine Analyse des Wärmetransports in einem dickwandigen durchströmten Rohr eingebracht. Es zeigt sich, daß die thermische Dispersionslänge bei den Fällen eines stationär aufgeprägten Temperaturgradienten und einer wandernden Temperaturwelle unterschiedlich sind. In beiden Fällen wird der Dispersionskoeffizient als Summe aus der statischen Wärmeleitfähigkeit und einem Term aufgrund der dispersiven Strömung definiert. Der Dispersionsterm ist dem Quadrat der Peclet-Zahl proportional. Es zeigt sich, daß der Proportionalitätskoeffizient von der Porosität, von den Stoffeigenschaften des Fluids und des Feststoffs und vom Temperaturfeld abhängt. Durch die Betrachtung eines Bündels von Rohren mit unterschiedlichem Radius wird der Einfluß von Heterogenitäten auf die thermische Dispersion ermittelt. Es zeigt sich, daß Änderungen des Porendurchmessers eine Zunahme der Dispersion um Größenordnungen bewirken. Ein Vergleich der Ergebnisse aufgrund des Dispersionsmodells mit veröffentlichten Versuchsdaten zeigt befriedigende Übereinstimmung.

## ТЕПЛОВАЯ ДИСПЕРСИЯ В ТОЛСТОСТЕННЫХ ТРУБАХ, ИСПОЛЬЗУЕМЫХ В КАЧЕСТВЕ МОДЕЛИ ПОРИСТОЙ СРЕДЫ

**Аннотация**—Теоретически исследуется тепловая дисперсия в пористых средах. В анализе теплопереноса в толстостенной трубе, содержащей поток жидкости, выявлен вклад распределений скорости на уровне пор в дисперсию. Показано, что в случаях стационарного температурного градиента и бегущей температурной волны возникает тепловая дисперсия разных видов. В обоих случаях коэффициент дисперсии определяется статической теплопроводностью и слагаемым, описывающим дисферсионное течение. Это слагаемое пропорционально квадрату числа Пекле. Показано, что коэффициент пропорциональности является функцией порозности, тепловых свойств жидкости и твердого тела, а также температурного поля. На примере пучка труб с различными ралиусами оценивается влияние неоднородностей на тепловую дисперсию. Показано, что изменения диаметров пор вызывают увеличения дисперсии на порядки. Получено удовлетворительное согласие между настоящей моделью дисперсии и опубликованными экспериментальными данными.